ELSEVIER

Catalysis Today 51 (1999) 501–511

CATALYSIS TODAY

Catalytic behavior of vanadium substituted mesoporous molecular sieves

Di Wei, Wei-Te Chueh, Gary L. Haller*

Department of Chemical Engineering, Yale University, New Haven, CT 06520, USA

Abstract

A series of V-MCM-41 samples with different pore sizes has been systematically investigated with both gas and liquid phase reactions. Methanol oxidation has been performed in the gas phase on these catalysts. Turnover frequencies are normalized by oxygen uptake measured under reaction conditions. A strong effect of pore size on the catalytic activity was observed in the form of a ''volcano curve'' and may be correlated with a variation in the local bond angle of Si–O–V. Considering this effect, the catalytic activity may be 'tuned' to maximum by varying the pore size. As expected, the same effect was observed in the liquid phase oxidation of cyclohexene. In order to interpret the pore size effect, the reaction rates of both the gas phase and liquid phase oxidation were then correlated with the variation of edge energies of V K-edge XANES on these MCM-41 catalysts. Additional reactions were performed in the liquid phase to compare the activity of V-MCM-41 with that of crystalline vanadium and titanium silicalite zeolites. The possible causes of the difference in the catalytic behaviors of these materials is also discussed.

Keywords: Vanadium substituted MCM-41; Pore size effect; X-ray absorption near edge structure (XANES); Methanol oxidation; Liquid phase oxidations

1. Introduction

Zeolites have had a great impact on catalytic science and technology. The success of zeolites in numerous industrial catalytic processes has stimulated the search for catalysts containing elements different from Al^{3+} in an ordered silica lattice. The idea of introducing foreign atoms into solids to change their catalytic properties is one of the main themes of heterogeneous catalytic research. However, in many cases these changes involve only the surface of the solid whereas the introduction of foreign atoms into the crystal lattice of a silica involves a change in the bulk structure. It was then discovered in the 1980s that the isomorphous substitution of certain transition metals into the zeolite lattice creates catalysts with remarkable catalytic activity for partial oxidation of hydrocarbons. Titanium incorporated silicalites such as TS-1 and TS-2 are known to be unique oxidation catalysts utilizing dilute hydrogen peroxide [1,2]. In addition to the hydrophobicity of the materials, the major role of the zeolite matrix is the stabilization of isolated redox centers. However, these materials are restricted to structures having pore diameters less than 13 Å. Large organic molecules are sterically hindered in zeolites, and this limits the usefulness of these catalysts to the oxidation of small organic compounds. The discovery of mesoporous molecular sieves was

*Corresponding author.

0920-5861/99/$ – see front matter
PII: S0920-5861(99)00036-X

immediately perceived as a possible solution to these limitations.

The new family of mesostructured molecular sieves MCM-41 was discovered in the early 1990s [3,4]. This material has a uniform, one-dimensional and hexagonal pore structure in the range 20–100 Å. It bridges the gap between crystalline zeolites and amorphous silica in terms of pore size and pore size distribution. The formation of MCM-41 has been rationalized by a liquid crystal templating (LCT) mechanism. Most importantly, the pore size may be varied in a systematic and predictable manner by changing the surfactant chain length.

Since MCM-41 was discovered, many efforts have been devoted to the further application of these uniform mesoporous materials. The initial modification was the incorporation of aluminum into the MCM-41 structure to create acidity [5,6] to catalyze alkylation [7] and hydrocracking [8] reactions. Shortly thereafter transition metals (Ti, V) were placed into the framework to obtain oxidation catalysts [9–12]. These transition metal incorporated MCM-41 materials, which have uniform mesopores, fulfill the requirements for catalyzing large molecules while retaining a uniform pore size.

Theoretically, the most important structural factor in zeolites is known to be the T–O–T bond angle [13]. The effect of chemical factors may be tested with many conventional zeolites with different cations for a given structure. However, there is no simple way to vary the T–O–T angle without also changing the structure of the zeolite. MCM-41 materials may provide such an opportunity.

In the present paper, after characterization of the structure of V-MCM-41 [14], we systematically investigated the pore size effect on catalytic behavior of these materials in the gas phase reaction utilizing molecular oxygen. Liquid phase oxidations were investigated by performing different reactions utilizing H_2O_2 and tert-butyl hydroperoxide (TBHP) as oxidants.

2. Experimental

The gases used in this study were helium (ultra-high purity grade 99.995%), oxygen (zero grade, 99.99%). The chemicals used in this study were methanol, acetonitrile and acetone (J.T. Baker), cyclohexene (Aldrich 99+%), cumene (Aldrich 99%), 1-hexene (Aldrich 99+%), phenol (Mallinckrodt, liquefied 89%, 11% H_2O), hydrogen peroxide (Fluka 35% in H_2O), and tert-butyl hydroperoxide (TBHP, Aldrich 90%, 10% H_2O).

2.1. X-ray absorption

X-ray absorption measurements were performed at NSLS Brookhaven National Laboratory at station X19A and X23A2, 2.5 Gev storage ring, using Si(1 1 1) monochromator crystal. Samples were pressed into self-supporting wafers and placed into a stainless steel cell, equipped with water cooled kapton windows, gas in- and outlet and heating unit allowed in situ treatment and reaction. Selected samples were subjected to in situ dehydration by heating to 350°C in 1 h and holding at this temperature for 1 h while purging with a helium/oxygen mixture.

In XANES analysis, following background removal (by victoreen fit) and normalization, the first inflection points of vanadium metal foil in the derivative spectra and of all samples are adjusted and aligned to 5465 eV. The relative edge energy positions were then calculated by taking the zero of energy with respect to this point.

2.2. Oxygen uptake

Oxygen uptake was performed in a computer controlled automatic flow system equipped with an online thermal conductivity detector (TCD). Samples (50–100 mg) were loaded into a Pyrex tube cell and held in place by glass wool. A four-way valve allowed switching between the pretreatment gas and carrier gas without disconnecting the sample cell. The oxygen chemisorption on V-MCM-41 samples was measured under reaction conditions by dosing very small amounts of oxygen over the catalyst samples. The catalysts were recalcined first at 500°C for 0.5 h in a mixed flow of helium and oxygen (5%). Then reduction was performed at 350°C in flowing methanol vapor (3% methanol, 97% helium). After reduction, a large flow of UHP helium was applied to remove the physisorbed methanol and further clean the catalyst surface. The catalysts were then exposed to a sequence of 1.6 μmol pulses of oxygen with a time interval of

1 min after the temperature had been reduced to the reaction temperature. The oxygen pulses were generated by a six-way valve and oxygen taken up by the samples was measured with the aid of TCD. Conditions for the reduction step (time, temperature) appeared to be close to asymptotes. Blank tests were also taken in the Pyrex cell (only glass wool inside) under the same pretreatment procedures and uptake conditions and showed no detectable O_2 uptake.

2.3. Methanol oxidation

The methanol oxidation was carried out in a computer controlled automatic reaction system. The reaction was performed in an isothermal fixed-bed downflow reactor operating at atmospheric pressure. The mass flow rate of methanol vapor was controlled by a vaporized liquid controller (TYLAN) while helium was bubbled through a methanol saturator. The vaporized liquid controller automatically adjusts the helium flow to maintain a constant flow rate of liquid vapor. The oxygen and another helium stream from two mass flow controller (Brooks) were then combined with the methanol vapor to give a reactant mixture of O_2 (3%), methanol vapor (3%) and helium (balance). The Pyrex glass reactor was held vertical with a ceramic gas distributor in the center. The outlet of the reactor to the gas chromatograph was heated to 423 K to avoid condensation of the products. The products were analyzed by an on-line gas chromatograph (HP-5700A) equipped with two TCDs and two columns (Porapack QS 80/100 packed column) connected in parallel. Blank runs were performed on the empty Pyrex reactor without any detectable conversions. Catalyst samples (200–500 mg, 60 mesh) were pretreated at 773 K for 0.5 h in an oxygen/helium mixture stream prior to each run. The oxidative dehydrogenation was then carried out over a 60 K temperature range (583–633 K). A series of varied flow rates of reactants were applied at each temperature to manipulate the measurements under different contact times.

2.4. Liquid phase reactions

Liquid phase reactions were carried out in a three-neck flask under reflux, heated in a mineral oil bath. A certain amount of solvent, oxidant and substrate was loaded and mixed well by stirring. The mixture was brought to reaction temperature before catalyst powder was added. Samples of 100 μl of reaction mixture were taken at selected reaction times, filtered and injected into a gas chromatograph (HP-6890 series) and analyzed by FID. After completion of the reaction, the catalyst was filtered and separated from the mixture. Hydrogen peroxide consumption was finally determined by iodometric titration. Reactions were also investigated under different solvent (methanol, acetonitrile or acetone) and different oxidant (hydrogen peroxide or tert butyl hydroperoxide – TBHP) conditions. Identification of hydrocarbons was performed in a GC–MS system (HP-5890 and HP5971A), and when necessary, the ^1H and ^{13}C NMR spectra were taken to confirm the species type.

3. Results and discussion

The synthesis and characterization of these V-MCM-41 samples were reported elsewhere [14]. The sample codes and basic physical properties are listed in Table 1.

3.1. Active sites

Oxygen uptake by the surfaces of pre-reduced catalyst samples has long been employed as a method for counting and differentiating among redox sites. Recently, Oyama and coworkers [15,16] have refined the conditions required to achieve consistent, plausible site-counting on vanadium oxide catalysts employed for the oxidative dehydrogenation of alcohols and other oxidation reactions. According to their work, sample reduction has to be controlled properly to avoid bulk reduction of the catalyst which would strongly affect the oxygen uptake measurements of

Table 1
The sample codes, synthesis and composition of V-MCM-41 samples

V-MCM-41 sample codes	Surfactants used	Si/V
VC8	$C_8H_{13}(CH_3)_3NOH$	~210
VC10	$C_{10}H_{13}(CH_3)_3NOH$	~210
VC14	$C_{14}H_{13}(CH_3)_3NOH$	~210
VC16	$C_{16}H_{13}(CH_3)_3NOH$	~210
VC16A	$C_{16}H_{13}(CH_3)_3NOH$	~700
VC16B	$C_{16}H_{13}(CH_3)_3NOH$	~1800

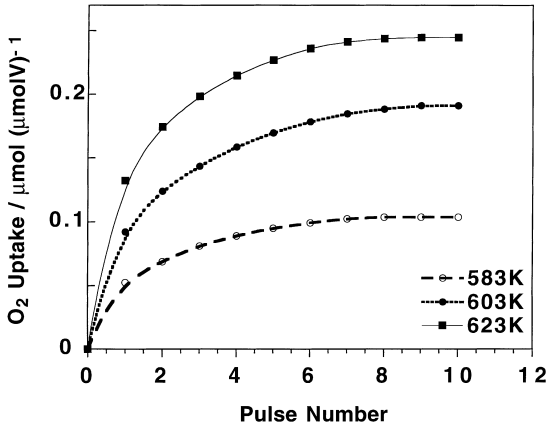

Fig. 1. O_2 uptake normalized by V sites after methanol reduction of VC16 sample. T reduction=T reoxidation.

active surface area. However, this is no longer a problem for the V-MCM-41 system because the pore wall of MCM-41 is so thin that essentially all vanadium atoms are surface sites. In the present case, more accurate results are obtained by reducing the catalyst directly by the reactant (methanol) and measuring the uptake by sending O_2 pulses under reaction conditions. This allowed us to count the actual sites participating in the reaction. A typical pattern of the oxygen chemisorption measured at different temperatures of methanol reduction (T_{ads}=T_{red}) was recorded on VC16 and shown in Fig. 1. The uptake has been normalized by vanadium concentration. Fig. 2 shows

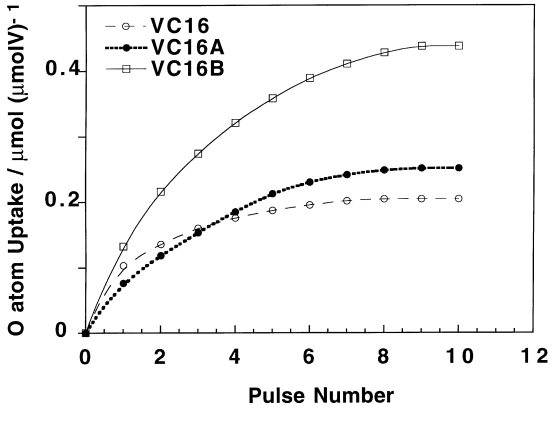

Fig. 2. Oxygen atom uptake normalized by V sites on samples with different V loading after methanol reduction at 583 K. The V loadings of these samples are: V16 (0.4 wt%); V16A (0.12 wt%); V16B (0.05 wt%).

oxygen atom uptake (normalized by V content) obtained on samples with different V loading after methanol reduction at 583 K. The maximum uptake per unit vanadium site increases as vanadium loading becomes lower and will approach unity at higher adsorption temperatures (the limiting stoichimetry of O/V=1). This suggests that lower metal loading results in higher fraction of isolated active sites in the methanol oxidation. There is no apparent trend in the amount of oxygen uptake observed in the samples with different pore sizes.

3.2. Gas phase reaction

Methanol oxidation in the gas phase has been investigated and used as a probe reaction on various vanadium catalysts such as supported vanadium oxides, etc. [17]. In the present study, the V-MCM-41 samples with different pore sizes were investigated systematically by this reaction. Methanol oxidation was generally used to produce formaldehyde with some byproducts such as CO, CO_2, H_2O and $(CH_3)_2O$. In order to determine the catalytic activity accurately, the reaction was measured at different contact times by varying the flow rate of reactants at each temperature. By taking the differential region in the correlation of total conversion versus contact time for every sample, we have been able to simplify the problem in comparing the reaction rates between different catalysts. The methanol (total) turnover frequencies (TOFs) have been calculated directly from the slope of the linear regime. Similarly, the TOFs to the main product (formaldehyde) has also been determined by using the linear regime of the correlation between the yield to formaldehyde versus contact time. This procedure assures that the turnover frequency remains constant under different conversions. Furthermore, the final reaction rates calculated have been normalized by the active sites which were determined by the oxygen uptake at corresponding temperatures under reaction conditions. Finally, the total TOFs and the TOFs to formaldehyde at varied temperatures are correlated with the pore size of V-MCM-41 samples and are shown in Figs. 3 and 4, respectively. The pore size of these V-MCM-41 samples have been calculated elsewhere [18] and showed a bimodel distribution. Here to simplify the case, the pore sizes have been determined based on that of silica MCM-41

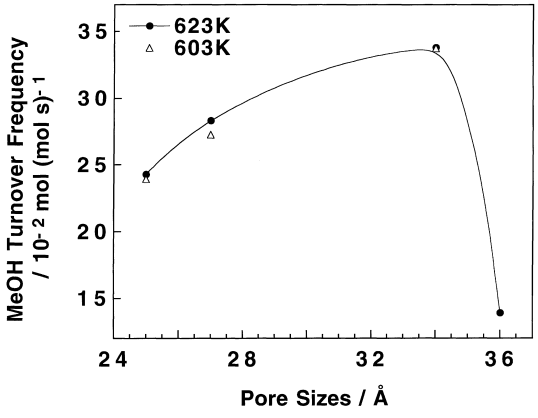

Fig. 3. The effect of pore size on methanol (total) turnover frequency normalized by oxygen uptake at various temperatures.

calculated by non-local density functional theory analysis of nitrogen physical adsorption since indeed there is only a slight decrease in the *d* spacing on V-MCM-41 samples.

3.3. Pore size effect

A strong effect of pore size on catalytic activity was observed on V-MCM-41 series samples. Interestingly, the effect is shown to be close to a "volcano curve" where the turnover frequency increased with increasing pore size to a maximum and then decreased. We assumed here that this phenomena may be related to

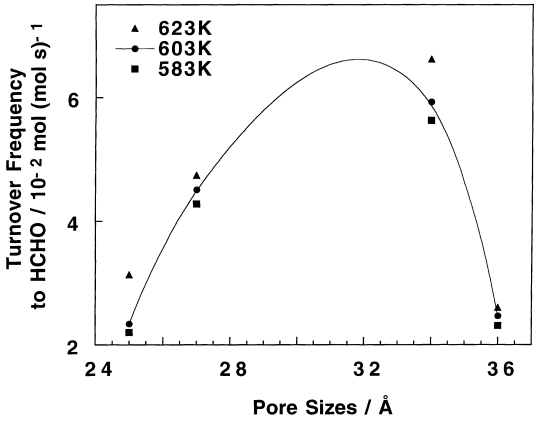

Fig. 4. The effect of pore size on the turnover frequency to formaldehyde normalized by oxygen uptake at various temperatures.

the change of local bond angles of Si–O–V as the nature of curvature of the pore wall changed. It is known that the most important structural factor in zeolites is the T–O–T angle. When the T–O–T angle is varied, the fundamental chemical variable is the change in the relative participation of *s*, *p* and *d* orbitals in the bonding. In the case of Al in most zeolites, the local crystal geometry is an important variable because it is related to acidity through the effect of this structural parameter on the Si–OH–Al bond angle. A similar effect is expected for Si–O–V bonds in V-MCM-41 samples. Considering the Si–OH–Al bond, the pore size effect is reflected in the acidity of the proton on the bridging hydroxyl. As for Si–O–V bond, this should be reflected in the oxidation potential of V which will quite naturally affect the activity of V in the catalytic oxidation. Another investigation by Haller and coworkers [19] did show that the acidity of alumina incorporated MCM41 was affected when the pore size was varied in the similar range.

3.4. Liquid phase reactions

Research activity on many oxidation reactions with H_2O_2 in the presence of V-containing silicalites has been carried out and reviewed [20]. Similar to titanium silicalites, isolated V sites in vanadium silicalites have been proposed to have a low activity for H_2O_2 decomposition. However, isolation alone is not sufficient to explain all the catalytic properties. The hydrophobic environment prevailing inside the catalyst pores and the multiple V–O–Si bonds that allow interaction with reactants but prevent complete hydrolysis of V sites in vanadium silicates must also play a role in stabilizing the dispersed V sites. V-MCM-41 materials which have a similar lattice V species and local environments to these silicalites, may share the same origin of catalytic activity in the presence of H_2O_2. Hydroxylation of phenol was the first reaction carried out on V-MCM-41, and indeed this reaction has become a standard for measurement of the activity and selectivity of different catalysts.

3.4.1. Hydroxylation of phenol

Phenol is oxidized to give catechol and hydroquinone in almost equal yield and high selectivity. After the initial discovery of the catalytic activity of TS-1

Table 2
A comparison between catalytic behavior of V-MCM-41 and that of titanium- and vanadium-containing silicalites in phenol hydroxylation

Catalysts	Si/V (Ti)	Conversion (%)	H_2O_2 conversion (%)	Product distribution (%)		
				HQ[a]	Catechol	*p*BQ[a]
TS-1[b]	34	27.0	100	50.0	49.0	1.0
V-MEL[c]	79	24.3	100	52	44.1	3.9
VC14[d]	210	4.6	100	77.2	2.7	7.5
VC16[e]	210	6.7	100	73.6	19.7	1.8

Note: Data on TS-1 and V-MEL were obtained from Ref. [20] and references therein.
[a] HQ: Hydroquinone; pBQ: *p*-benzoquinone.
[b] TS-1: catalyst weight=0.72 g, phenol=0.22 mol, phenol/H_2O_2 (mol)=3.8, T=373 K, reaction duration=1 h, solvent=water/acetone.
[c] V-MEL: catalyst weight=0.1 g, phenol=0.011 mol, phenol/H_2O_2 (mol)=3, T=342 K, reaction duration=29 h, solvent=acetone.
[e] V-MCM-41: VC14 (C_{14}-surfactant), catalyst weight=0.4 g, phenol=18 mmol, phenol/H_2O_2 (mol)=3, T=352 K, reaction duration=5 h, solvent=acetonitrile.
[f] V-MCM-41: VC16 (C_{16}-surfactant), catalyst weight=0.4 g, phenol=0.035 mol, phenol/H_2O_2 (mol)=2.5, T=351 K, reaction duration=5 h, solvent=acetonitrile.

for this reaction [1], other transition metal containing zeolites such as V-MEL and TS-2 have been found to be effective catalysts. The results reported for phenol hydroxylation on V-MEL are comparable with those reported for TS-1 [20]. The best results on TS-1, 94% selectivity based on phenol and 84% based on H_2O_2 at 30% conversion of the phenol, can be obtained only when all the reaction conditions are optimized [21]. Table 2 summarizes the results of phenol hydroxylation on V-MCM-41 samples (VC14 and VC16) with reaction conditions recorded as notes. A comparison is also made between the catalytic behavior of V-MCM-41 and that of titanium- and vanadium containing silicalites reported in the literature [20]. Compared with these silicalites, much (4–5 times) lower conversion of phenol was observed on our V-MCM-41 samples. The yield to hydroquinone and catechol is also not equal, but instead, much higher selectivity to hydroquinone is obtained. In contrast, the H_2O_2 conversion is 100% under all conditions for all samples. Now the question arises as to what the possible causes are for the much lower activity observed on the V-MCM-41 samples than that on vanadium silicalites, even though they share quite similar local environments.

3.4.2. 1-Hexene oxidation

Olefins are usually selectively oxidized to obtain the corresponding epoxide products. 1-Hexene was used first as the substrate to detect the intrinsic activity of V-MCM-41 catalysts since the molecular size of 1-hexene avoids diffusion limitations in the oxidation. This reaction was performed on sample VC14 at 333 K with H_2O_2 in acetonitrile. The main product has been identified as hexane-1,2-diol and the selectivity to the desired epoxide is quite low. The formation of hexane-1,2-diol may be due to a further hydrolytic reaction of the epoxide. The results are summarized in Table 3 and compared with the titanium silicalites reported by Notari [21]. The catalytic activity of the V-MCM-41 sample is far below the medium-pore TS-1 and large-pore Ti-Beta. The selectivity to epoxide on V-MCM-41 is very close to that on large-pore Ti-Beta but much lower than that on TS-1. As pointed out by Corma et al. [11], because of the high concentration of silanol groups in MCM-41 samples, the hydrophobicity is lower than that of silicalites. The hydrophobic–hydrophilic characteristics of the samples may play a role in the different catalytic behavior. The advantages of using of mesoporous materials instead of zeolites may be seen when large organic molecules like cyclohexene are to be oxidized.

3.4.3. Cyclohexene oxidation

Cyclohexene is oxidized very slowly to epoxide product in the presence of TS-1. This low reactivity has been attributed to the molecular dimensions of cyclohexene, which cannot enter the channel system of TS-1. When Ti-beta and Ti-MCM-41 are used as the catalysts, cyclohexene can be oxidized by H_2O_2 and even TBHP for the latter [11]. In the present study,

Table 3
A comparison between catalytic behavior of V-MCM-41 and that of titanium-containing silicalites in 1-hexene epoxidation

Catalysts	TON (s^{-1})[a]	H_2O_2 Conversion (%)	Epoxide selectivity (%)
TS-1	50.0	98	96
Ti-Beta	12.0	80	12
VC14[b]	0.1	98	11.5

Note: Data on TS-1 and Ti-Beta were obtained from Ref. [21] and references therein.
[a] TON: Turnover number of 1-hexene.
[b] V-MCM-41: VC14 (C_{14}-surfactant), catalyst weight=0.20 g, 1-hexene=35 mmol, 1-hexene/H_2O_2 (mol)=3, T=333 K, reaction duration=1 h, solvent=acetonitrile.

cyclohexene oxidation was investigated carefully over the series of V-MCM-41 samples using different solvents and oxidants (H_2O_2 and TBHP).

Solvents generally affect the catalytic activity and selectivity in liquid phase reactions. Different solvents result in a different distribution of products. The solvent effect was studied here by reacting cyclohexene with H_2O_2 in methanol, acetone and acetonitrile. The cyclohexene can be oxidized over V-MCM-41 catalysts to a number of products including cyclohexene epoxide; 1,2-cyclohexanediol; cyclohexenyl hydroperoxide; cyclohexanol and 2-cyclohexen-1-one, etc. The results of cyclohexene conversion and product distribution under different solvents are summarized in Table 3. In the case of aprotic solvents such as acetone and acetonitrile, the highest selectivity goes to cyclohexenyl hydroperoxide. Cyclohexenyl hydroperoxide as a major product of cyclohexene oxidation has not been reported in the literature. To confirm this product, GC–MS analysis, ^{13}C-NMR and ^{1}H-NMR measurements were carefully performed. Furthermore, the effect of pore size on the catalytic behavior of V-MCM-41 was also studied by this reaction.

3.5. Pore size effect

In order to simplify the calculation, similar to the gas phase reaction, the turnover frequency (TOF) has been derived from the linear regime of the reaction curve. A typical pattern of the reaction curve is recorded on VC16 and shown in Fig. 5. This TOF was then normalized by the total vanadium content to obtain the final reaction rate. Fig. 6 plots the correlation between pore size and the cyclohexene (total) TOF and the TOF to cyclohexenyl hydroperoxide. As might be expected, the total TOF and TOF to the main product follows the same trend as observed in the gas phase reaction for V-MCM-41 samples.

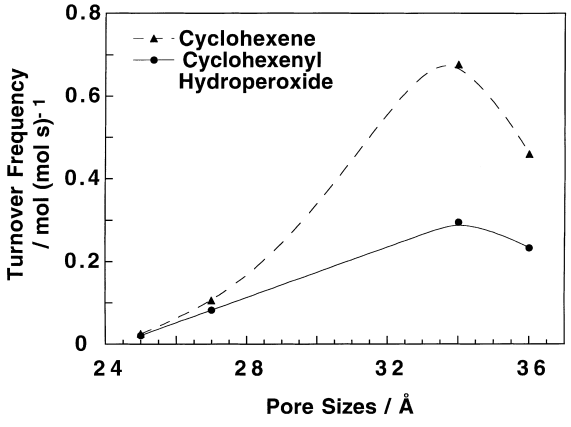

Fig. 5. The conversion of cyclohexene and yield to cyclohexenyl hydroperoxide versus reaction duration on VC16 in the presence of H_2O_2 at 333 K with acetonitrile as solvent.

The "volcano curve" is usually caused by the difference in the strength of adsorption bond with reactants. The bond strength is closely related to the electron density of the active metal site. Indeed, the strong repulsion between formally unshared electrons in planar H_2O_2 can be reduced by transition-metal ions such as V^V, as they accept electron density from the

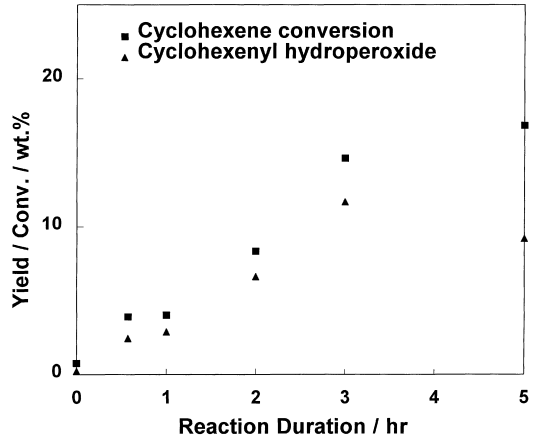

Fig. 6. The effect of pore size on cyclohexene (total) turnover frequency (TOF) and the TOF to cyclohexenyl hydroperoxide at 333 K.

filled antibonding orbitals of H_2O_2 interacting with the empty metal d orbital of appropriate symmetry. On the other hand, the electronic state of V site in V-MCM-41 framework may be reflected in the X-ray absorption near edge structure (XANES). The first row transition elements have well-defined site symmetry spectra in the XANES. The relative position of the pre-edge peak and K-absorption edge of an element is governed by its chemical state. The energy shift of the edge, the so called chemical shift, is primarily the result of the effective charge on the absorbing atom, but its value is also sensitive to the detailed electronic configuration of the valence band in the absorbing atom. In other words, the energy shift should represent the shift in electron density of the absorbing atom. According to Wong [22], the energy shift is found to follow Kunzl's law and to vary linearly with the valence of the absorbing vanadium atom. The positive shift in the threshold energy corresponds to a valence increase. More generally, a positive shift of edge energy suggests a decreasing electron density on the atom.

In the present case, the V K-edge energies determined by XANES measurements under hydrated and dehydrated conditions are correlated with the pore size of V-MCM-41 samples. As shown in Fig. 7, the edge energies decrease linearly with the increasing pore size. A positive shift of edge energy was observed upon dehydration, indicating a decreasing electron density on V atom. This may possibly be caused by the loss of water as an electron donor. Moreover, by varying the pore size, the electron density of the V site could probably be tuned through a variation of the local bond angles.

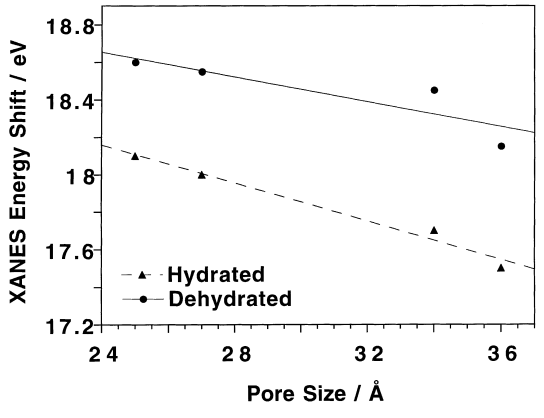

Fig. 7. The correlation of V K-edge energies measured on hydrated and dehydrated V-MCM-41 samples with the pore size.

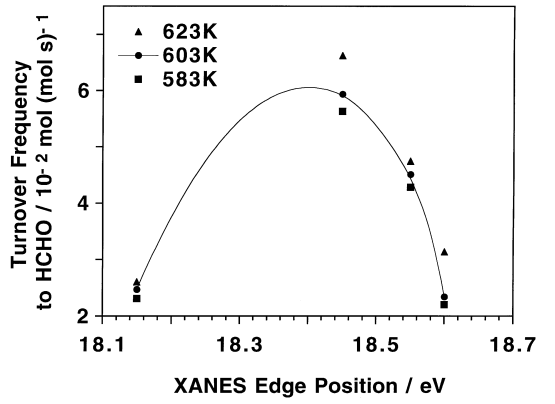

Fig. 8. The reaction rates of methanol oxidation varied with the edge energy measured on dehydrated V-MCM-41 samples.

Meanwhile, a correlation in Fig. 8 shows the reaction rates of methanol oxidation varied with the edge energy (dehydrated condition – since methanol oxidation was carried out after the recalcination of the catalysts at 773 K) to present essentially a ''volcano curve''. Fig. 9 shows the same trend in a correlation of reaction rates of cyclohexene oxidation with the edge energy obtained under hydrated condition (since the oxidation occurred over hydrated samples in the liquid phase). It is thus proposed that the electron density of V sites, which may be ''tuned'' by the pore size through a variation of Si–O–V bond angles, will quite naturally affect the effective redox potential of V sites

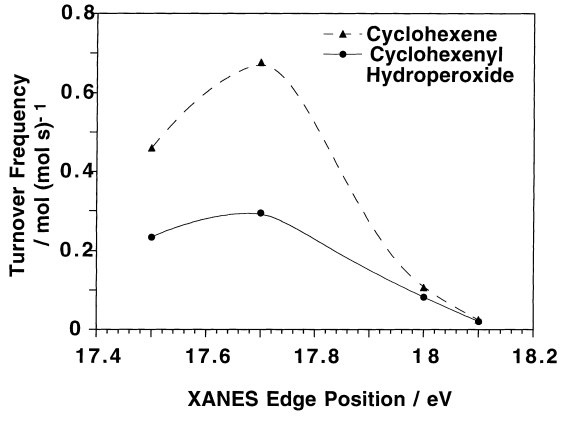

Fig. 9. The reaction rates of cyclohexene oxidation varied with the edge energy measured on hydrated V-MCM-41 samples.

Table 4
Product distribution of cyclohexene oxidation catalyzed by V-MCM-41 (VC14) with different solvents and oxidants

Solvents/oxidants	Conversion (%)	H_2O_2 conversion (%)	Product distribution (%)					
			EP[a]	CyHP[a]	2-ol[a]	1-one[a]	1,2-diol[a]	Others
Acetonitrile[b]	42.7	73	5.9	42.5	19.3	8.3	7.5	16.5
Acetone[b]	32.1	90	2.7	28.7	19.6	14.8	8.0	26.2
Methanol[c]	58.6	99	1.0	0.0	12.2	22.6	12.2	52.0
TBHP[d]	21.1	–	20.4	30.9	0.4	1.8	2.0	26.5

Note: [a] EP: Epoxide; CyHP: Cyclohexenyl hydroperoxide; 2-ol: 2-cyclohexanol; 1-one: 2-cyclohexene-1-one; 1,2-diol: cyclohexane-1,2-diol.
[b] Catalyst weight=0.07 g.
[c] Catalyst weight=0.20 g; cyclohexene=0.035 mol, cyclohexene/H_2O_2 (mol)=5, T=333 K, reaction duration=5 h.
[d] Catalyst weight=0.07 g; cyclohexene=0.035 mol, cyclohexene/H_2O_2 (mol)=1, T=333 K, reaction duration=5 h.

and further affect the adsorption bond strength. With regard to the theory of the ''volcano curve'', the maximum activity is exhibited for the metal for which reactants presumably have an intermediate strength of adsorption, which is in consonance with the general idea that the fastest rate is achieved when the bonds between the adsorbed intermediate complex and the catalyst are neither too strong nor too weak.

3.6. Reaction mechanism

According to Satterfield [23], the behavior of most oxidation catalysts can be interpreted within the framework of a redox mechanism (reduction–oxidation). This postulates that the catalytic reaction comprises two steps: 1. Reaction between catalyst in an oxidized form Cat-O, and hydrocarbon R, in which the oxide becomes reduced: Cat-O+R→RO+Cat. 2. The reduced catalyst, Cat, becomes oxidized again by oxygen from the gas phase: 2Cat+O_2→2Cat-O. Under steady-state conditions, the rates of the two steps must be the same.

The radical mechanism has been proposed as a general mechanism for oxidation of alkenes and aromatics. According to Mimoun et al. [24], the formation of vanadium peroxo radical is believed to be the active species for the transfer of oxygen to the reactants in the liquid phase oxidation using H_2O_2. Thus, the transferred oxygen atom now is of a peroxidic nature. The reduction of the V^{5+} to V^{4+} is required for the formation of the peroxo radical, which is favored by highly dispersed V in molecular sieves. The vanadium (V^{IV}–O–O$^{\bullet}$) peroxo radical can both epoxidize olefins and hydroxylate alkanes and aromatic hydrocarbons. Epoxidation of cyclohexene would proceed upon the homolytic addition of (V^{IV}–O–O$^{\bullet}$) to the double bond, giving a free radical intermediate which homolytically decomposes to give the epoxide and vanadium oxo compound. In the present case, epoxidation is only a minor reaction, instead like hydroxylation, a hydrogen atom was probably abstracted by (V^{IV}–O–O$^{\bullet}$) to give an intermediate carbon radical followed by a recombination with V–OOH to give a hydroperoxide product. It is not well understood why this happened to be the major reaction. However, it may be related to initial coordination of reactants to the vanadium center and also the water content present in the reaction using H_2O_2. When the oxidant was switched to TBHP, a significant increase in the selectivity to epoxide product was observed as shown in Table 4.

3.7. Cumene oxidation

As observed from the cyclohexene oxidation with H_2O_2 in acetonitrile, the main product has been identified as cyclohexenyl hydroperoxide on V-MCM-41 samples. On the other hand, cumene hydroperoxide has been an important industrial intermediate to produce phenol [25]. Accordingly, cumene oxidation in acetonitrile by utilizing H_2O_2 was carried out on VC16 at 343 K. The reaction conditions and results are recorded in Fig. 10 and the conversion of hydrogen peroxide approach 100% after 6 h. The reaction conditions still need to be optimized to reach higher conversion and selectivity.

4. Summary

The catalytic properties of V-MCM-41 catalysts have been investigated carefully by both gas and liquid

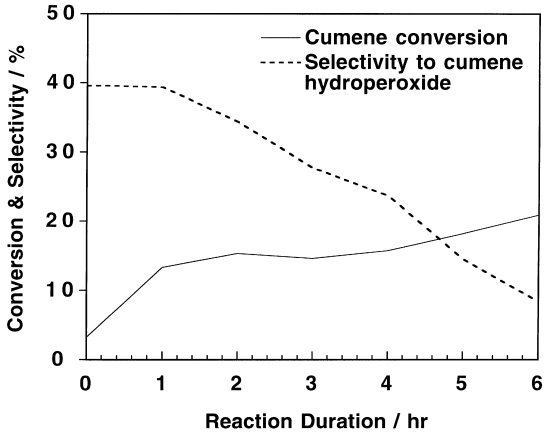

Fig. 10. Cumene oxidation on VC16: catalyst weight=0.2 g; cumene=0.035 mol, cumene/H_2O_2 (mol)=2.5, T=343 K, reaction duration=5 h, solvent=acetonitrile.

phase oxidations. Oxygen uptake measured under reaction conditions provided a method of in situ counting of the active sites in the gas phase oxidation. More importantly, a strong effect of pore size was observed on the catalytic behavior of V-MCM-41 samples and was assumed to be related to the variation of local Si–O–V bond angles. The electron density of V sites which was reflected by V K-edge energy in XANES, may possibly be ''tuned'' through a variation in the bond angles which could be realized by varying the pore size. Further correlations between V K-edge energy and reaction rates of both the gas and liquid phase oxidations present a ''volcano curve''. The effective redox potential was adjusted to the maximum when the intermediate adsorption bond strength was formed between active V sites and reactants.

Another important observation is that the catalytic activity of V-MCM-41 in the presence of H_2O_2 is far below that of titanium- or vanadium-silicalites. Diffusion limitations and steric constraints due to reactants or transition-state intermediates are not the only factors that govern the activity of active metal sites in molecular sieves. As pointed out by Sayari [26], the reason for a strong dependence of catalytic properties on the nature of the silicate matrix is not well understood. Indeed, none of the spectroscopic techniques used so far including X-ray absorption shows any difference in the local environment of Ti (V) in various crystalline silicates and MCM-41. Decreased hydrophobicity MCM-41 material may be a contributing factor in the decrease of the intrinsic catalytic activity of metal sites. However, he suggested that subtle variations of some important properties such as bond angles or redox potential may be at the origin of this behavior.

To find an answer to the above observation, the acidity performance of zeolites and amorphous materials are considered. The amorphous silica alumina was found to be less acidic than most of the zeolites. In other words, the affinity of protons would be highest in the amorphous state when the Si–O–Al bonds are connected in the most ''comfortable'' angles and they are thermodynamically most stable. While in the case of zeolites, because of the rigid crystalline framework and pore structure, the Si–O–Al bonds are connected in restricted angles and thermodynamically they are less stable than those of amorphous materials. Therefore, the acidity would be higher for zeolites because of the lower affinity of the protons.

Considering the case of the oxidation catalysts, which were synthesized by substituting vanadium or titanium into MCM-41 and the silicalite frame work, the crucial difference in the structure of MCM-41 and silicalite is that the MCM-41 material has no long range order and the pore walls are essentially amorphous. The Si–O–V (Ti) bonds sitting in the amorphous environment of MCM-41 are supposed to be connected by more ''comfortable'' bond angles and are thermodynamically more stable than those of vanadium or titanium incorporated silicalites, which have a crystalline framework. Therefore the V (Ti)–O–Si bonds in MCM-41 should be less reactive and have lower redox potential than those in silicalite samples. By utilizing TBHP, Corma and coworkers [11] performed the oxidation of 1-hexene on Ti-MCM-41 and amorphous Ti-SiO_2, respectively, since H_2O_2 decomposes and is not an active oxidant on amorphous Ti-SiO_2. He found that activity per Ti atom turns out to be the same for both materials. The explanation given here based on bond angle effect may provide an explanation for why the activity of V (Ti) incorporated MCM-41 is much lower than that of V (Ti) incorporated silicalite, even though the local environments are quite similar.

Acknowledgements

We would like to acknowledge the financial support from DOE Office of Basic Energy Sciences and NSF.

We also thank NSLS Brookhaven National Laboratory for beam time. The assistance of Drs. Shuji Tanabe and Robert Weber in the construction and use of the automated gas phase reactor is gratefully acknowledged. GLH wishes to thank the Northwestern University Surface Science and Catalysis Center, where a preliminary comment was published in the Center News Letter while he was VN Ipatieff Lecturer.

References

[1] M. Taramasso, G. Perego, B. Notari, US Pat. 4 410 501 (1983).
[2] J.S. Reddy, R. Kumar, P. Ratnasamy, Appl. Catal. 58 (1990) L1.
[3] C.T. Krege, M.E. Leonowicz, W.J. Roth, J.C. Vartuli, J.S. Beck, Nature 359 (1992) 710.
[4] J.S. Beck, J.C. Vartuli, W.J. Roth, M.E. Leonowicz, C.T. Kresge, K.D. Schmitt, C.T-W. Chu, D.H. Olson, E.W. Sheppard, S.B. McCullen, J.B. Higgins, J.L. Schlenker, J. Am. Chem. Soc. 114 (1992) 10834.
[5] Z. Luan, C.-F. Cheng, W. Zhou, J. Klinowski, J. Phys. Chem. 99 (1995) 1018.
[6] A. Corma, V. Fornes, M.T. Navarro, J. Pérez-Pariente, J. Catal. 148 (1994) 569.
[7] E. Armengol, M.L. Cano, A. Corma, H. Garcia, M.T. Navarro, J. Chem. Soc., Chem. Commun. (1995) 519.
[8] A. Corma, A. Martinez, V. Matinez-Soria, J.B. Monton, J. Catal. 153 (1995) 25.
[9] K.M. Reddy, I. Moudrakovski, A. Sayari, J. Chem. Soc., Chem. Commun. (1994) 1491.
[10] A. Corma, M.T. Navarro, J. Pérez-Pariente, J. Chem. Soc., Chem. Commun. (1994) 147.
[11] T. Blasco, A. Corma, M.T. Navarro, J. Pérez-Pariente, J. Catal. 156 (1995) 65.
[12] T.Kr. Das, K. Chaudhari, A.J. Chandwadkar, S. Sivasanker, J. Chem. Soc., Chem. Commun. (1995) 2495.
[13] R.A. van Santen, Theoretical Heterogeneous Catalysis, World Scientific, Singapore, 1991, pp. 352–369.
[14] D. Wei, H. Wang, X. Feng, W. Chueh, P. Ravikovitch, M. Lyubovsky, T. Takehuchi, G.L. Haller, J. Phys. Chem. (1999), in press.
[15] S.T. Oyama, G.T. Went, K.B. Lewis, A.T. Bell, G.A. Somorjai, J. Phys. Chem. 93 (1989) 6786.
[16] S.T. Oyama, G.A. Somorjai, J. Phys. Chem. 94 (1990) 5022.
[17] G. Deo, I.E. Wachs, J. Catal. 146 (1994) 323.
[18] P.I. Ravikovitch, D. Wei, W. Chueh, G.L. Haller, A.V. Neimark, J. Phys. Chem. B 101 (1997) 3671.
[19] X. Feng, J. Lee, J.W. Lee, J.Y. Lee, D. Wei, G.L. Haller, Chem. Eng. J. 64 (1996) 255.
[20] G. Bellussi, M.S. Rigutto, Stud. Surf. Sci. Catal. 85 (1994) 177.
[21] B. Notari, in: D.D. Eley, W.O. Haag, B.C. Gates (Eds.), Advances in Catalysis, vol. 41, Academic Press, New York, 1996, p. 253.
[22] J. Wong, F.W. Lytle, R.P. Messmer, D.H. Maylotte, Phys. Rev. B 30 (1984) 5596.
[23] C.N. Satterfield, Heterogeneous Catalysis in Industrial Practice, 2nd ed., McGraw-Hill, New York, 1991, p. 269.
[24] H. Mimoun, L. Saussine, E. Daire, M. Postel, J. Fischer, R. Weiss, J. Am. Chem. Soc. 105 (1983) 3101.
[25] H.-J. Arpe, in: K. Weissermehl (Ed.) Industrielle Organische Chemie, VCH Verlagsgesellschaft mbH, Weinheim, 1988.
[26] A. Sayari, Stud. Surf. Sci. Catal. 102 (1996) 1.